

Preparation of Chitosan/Organoclay Nanocomposite as Silver(I) Ion Adsorbent

WALAIKORN NITAYAPHAT^{1,*} and THANUT JINTAKOSOL²

¹Department of Home Economics, Faculty of Science, Srinakharinwirot University, Bangkok, Thailand

²Department of General Science, Faculty of Science, Srinakharinwirot University, Bangkok, Thailand

*Corresponding author: Fax: +66 2 2584000; Tel: +66 2 6495000; E-mail: walaikorn@g.swu.ac.th

Received: 23 September 2016;

Accepted: 5 November 2016;

Published online: 30 December 2016;

AJC-18227

Different molecular weight chitosans were prepared by the depolymerization of commercial chitosan with hydrogen peroxide. The depolymerized chitosans were used to modify montmorillonite to provide organoclay. The chitosan/organoclay nanocomposite beads were evaluated as an adsorbent of Ag(I) ion. Batch adsorption experiments were performed as a function contact time, organoclay concentration, pH and adsorbent dosage. Isotherm analysis showed that the adsorption pattern of Ag(I) ion onto nanocomposite followed well the Langmuir model. Using the Langmuir model equation, the maximum adsorption capacity of nanocomposite bead was found 80.39 mg g⁻¹. The pseudo-second order equation described best kinetic data of Ag(I) ion. The Ag(I) ion desorption of nanocomposite bead was 9.68 % at pH 4. SEM/EDX images confirm that after adsorption the Ag(I) ions were dispersed onto the nanocomposite bead surface. This study demonstrated that the chitosan/organoclay nanocomposite can effectively remove Ag(I) ion from aqueous solution.

Keywords: Chitosan, Organoclay, Nanocomposite, Silver, Adsorbent.

INTRODUCTION

Production and consumption of silver is increasing continuously worldwide. According to World Silver Survey 2015, excessive amounts of silver reaching up to 1.07 billion ounces are consumed worldwide. The major industrial sources of silver released into the environment are photographic film manufacturing, mirroring, electroplating, antimicrobial materials, batteries, catalyst, coinage, jewelry and medication industries due to its excellent properties such as antimicrobial, ductility, electrical and thermal conductivity, malleability and photo-sensitivity [1]. Therefore, silver ion pollution in wastewater is caused by these industrial activities. The contact with soluble silver compounds may cause several negative health effects such as corneal injury, skin irritation, liver and kidney damage, stomach pain and changes in blood cells [2,3]. The toxicity and high value of silver result in the effective removal and recover of silver has become an urgent assignment. Adsorption represents an effective and simple technique to remove both inorganic and organic micro-pollutants. Natural biopolymers are gaining interest for application as adsorbents in wastewater treatment because their biodegradability and non-toxicity [4].

Natural clay minerals have been widely used for many years as inorganic filler for plastics and rubbers to reduce the polymer consumption and cost. Because of their low cost, abundance in natural, excellent absorptivity and potential for

ion-exchange, clay minerals are strong candidates as adsorbents [5]. The most commonly used clay is montmorillonite (MMT) because of its high cation exchange capacity (CEC), great surface area, swelling behaviour and strong adsorption ability [6-9]. Montmorillonite, which is a 2:1 layered aluminosilicate, consist of two silica tetrahedral sheets attached to a central Al octahedral sheet. It has stable negative charges. The surface of montmorillonite is hydrophilic due to inorganic cations, such as Na⁺ and Ca²⁺, become strongly hydrated in the presence of water. As a result, the adsorption ability of organic pollutants on natural montmorillonite is very low [10,11]. Thus, attempts have been made to improve the adsorption capacity of montmorillonite. One strategy is to modify the clay mineral surface with a cationic surfactant such as alkyl ammonium salts [12]. Replacement of exchangeable cations with cationic surfactants changes the surface of clay minerals from hydrophilic to a hydrophobic and the obtained complex is an organoclay [12,13]. In consequence of the modification of the clay, the surface properties change from highly hydrophilic to increasingly hydrophobic [14]. Such organoclays can be used as adsorbents for the removal of organic substances [15-17]. Chitosan (CTS), a natural polyaminosaccharide synthesizes from the deacetylation of chitin, has been reported to be a suitable biopolymer for the removal of heavy, transition metal and dyes from wastewater due to it contain amino and hydroxyl groups that serve as the active sites of interaction [18-20].

In this study, chitosan/organoclay nanocomposite beads were prepared by blending chitosan with montmorillonite modified by depolymerized chitosan to provide organoclay. The adsorption efficiency, isotherms and kinetics for Ag(I) ion from aqueous solution onto nanocomposite were evaluated.

EXPERIMENTAL

Commercial grade high molecular weight chitosan with an average molecular weight of 150 kDa and 90 % degree of deacetylation, (CTS_{initial}), was purchased from Seafresh Chitosan (Lab) Co., Ltd. (Thailand). Hydrogen peroxide 30 % (v/v), purchased from Merck Ltd. (Thailand), was used to depolymerize chitosan. Sodium montmorillonite with a cation exchange capacity (CEC) of 50 meq/100 g and a moisture content of 8-12 % was supplied from Thai Nippon Chemical Industry Ltd. (Thailand). Silver nitrate (AgNO₃), sodium hydroxide, hydrochloric acid and acetic acid (analytical grade) was purchased from Merck Ltd. (Thailand).

Preparation of depolymerized chitosan: The depolymerized chitosan was prepared by dissolving 5 g of high molecular weight chitosan in 100 mL of H₂O₂ solution at room temperature with two different H₂O₂ concentrations [10 and 20 % (v/v)] for either 12 or 24 h. After the reaction, each sample was filtered to remove the foam and undissolved impurities, washed with distilled water until the filtrate was neutral and then dried at 50 °C for 12 h.

Preparation of organoclay: The aqueous solution of CTS_{initial} was prepared by dissolving 2 g of original chitosan in 50 mL of 2 % (v/v) acetic acid solution and stirred with a magnetic stirrer for 1 h. Montmorillonite (2.5 g) was dispersed in 50 mL of distilled water and stirred for 1 h. The chitosan solution was then added to the montmorillonite dispersion and the mixture was stirred at 2000 rpm in a hi-speed mixer at room temperature for 1 h to separate the organoclay from the solution. The precipitate was washed with distilled water and then dried at 70 °C for 24 h, prior to being ground and sieved through a 200 mesh sieve. In addition to CTS_{initial}, the four depolymerized chitosans, CTS₂₈, CTS₂₅, CTS₂₄ and CTS₁₈, were used to prepare using same procedure.

Preparation of chitosan/organoclay nanocomposite beads: Pure chitosan beads were prepared by dissolving 2 g of chitosan powder (CTS_{initial}) in 50 mL of 2 % (v/v) acetic acid solution and stirring for 1 h at room temperature. This mixture was dropped through a syringe into a precipitation bath containing an alkaline coagulating mixture (H₂O:C₂H₅OH:NaOH = 4:5:1, w/w) gave rise to the chitosan beads.

Chitosan solution was obtained by dissolving chitosan in 2 % (v/v) aqueous acetic acid solution. Organoclay was slowly added to the chitosan followed by stirring for 1 h at room temperature to prepare chitosan/organoclay nanocomposites, in which the concentrations of organoclay were 1 wt % (chitosan/organoclay-1), 2 wt % (chitosan/organoclay-2), 3 wt % (chitosan/organoclay-3), 4 wt % (chitosan/organoclay-4) and 5 wt % (chitosan/organoclay-5), respectively. The mixtures were stirred with sonication for 6 h at room temperature. Then, the mixtures were dropped through a syringe into a precipitation bath gave rise to the chitosan/organoclay nanocomposite beads. The beads were extensively washed with de-ionized water and preserved in an aqueous environment for further use.

Characterization: The molecular weight of chitosan was characterized by Gel Permeation Chromatography (Water, Water 600E). X-ray diffraction (XRD) patterns of the organoclay were performed using a Bruker AXS model D8 Diffractometer at 40 kV and 40 mA. The diffraction curves were obtained from 3 to 40° at a scanning rate at 0.02°/min.

The surface morphology of chitosan and chitosan/organoclay nanocomposite beads were obtained from the scanning electron microscopy (SEM) using a JEOL JSM-6335F microscope. Energy dispersive X-ray spectroscopy (EDX, Oxford) was applied to confirm existence and distribution of specific elements onto chitosan and chitosan/organoclay nanocomposite beads.

Batch adsorption procedure: Batch adsorption experiments were carried out by using chitosan and chitosan/organoclay nanocomposite samples (with different organoclay concentration) as adsorbents. The standard Ag(I) ions solution (10 mg L⁻¹) was prepared from AgNO₃. Atomic absorption spectroscopy (AAS, Analyst 300) was used for the determination of Ag(I) ions.

Several preliminary batch experiments were performed for determination of organoclay concentration in bead, contact time, optimum pH and adsorbent dosage. For a typical adsorption experiment, 1 g adsorbent was dispersed in 100 mL of 10 mg L⁻¹ AgNO₃ solution without adjusting the pH value. The dispersion was shaken at a speed of 100 rpm at 30 °C. For optimization of contact time to achieve maximum adsorption efficiency, batch adsorption experiments were realized at various times changed between 0 and 240 min. The initial pH values of solution (in the range of 4 to 10) were adjusted with 0.1 M NaOH or 0.1 M HCl. The effect of adsorbent dosage on the adsorption efficiency was studied at interval of 1 to 5 g.

Adsorption isotherms: The procedure for carrying out adsorption isotherm tests was as follows: a series of 250 mL flasks were employed. Each flask was filled with 100 mL of AgNO₃ solution of varying concentrations and the pH was adjusted to 4. One gram of adsorbent was added into each flask and shaken continuously at a speed of 100 rpm at 30 °C for 150 min. The quantity of Ag(I) ions adsorbed was derived from the concentration change.

Adsorption kinetics: The adsorption kinetics of chitosan and chitosan/organoclay nanocomposite beads for Ag(I) ions were conducted with 100 mL AgNO₃ solutions of concentrations (2, 4, 6, 8 and 10 mg L⁻¹), maintained at pH 6, temperature 30 °C at different contact time of 0-150 min. the adsorption capacity for Ag(I) ions uptake, q_e (mg g⁻¹), was determined as follows:

$$q_e = (C_0 - C) \frac{V}{W} \quad (1)$$

where C₀ and C are the initial and final concentrations (mg L⁻¹), respectively. V is the volume of solution (L) and W is the weight of adsorbents (g).

Desorption studies: Desorption of Ag(I) ions in batch system was evaluated in this study. First, adsorption experiments were carried out under the optimum batch conditions: at initial pH 6, contact time 150 min and temperature 30 °C. For desorption process, the adsorbent used in prior stage was washed with deionized water to remove any unadsorbed Ag(I)

ions. The desorption experiment was determined in the pH range from 4 to 10 with a constant stirring (100 rpm) at 30 °C for 150 min.

RESULTS AND DISCUSSION

Characterization of the depolymerized chitosan: The average molecular weight and polydispersity of depolymerized chitosans are shown in Table-1. It was found that the concentration of H₂O₂ and the reaction time are important factor affecting the average molecular weight and polydispersity of depolymerized chitosans. The higher concentration of H₂O₂ and the longer reaction time both provided a lower molecular weight of depolymerized chitosan. Therefore, 20 % (v/v) H₂O₂ for 24 h provided the lowest \bar{M}_w and \bar{M}_n and also polydispersity of depolymerized chitosan.

Interlayer separation of montmorillonite by depolymerized chitosan: The modified montmorillonite with different molecular weight of chitosan (CTS_{initial}, CTS₂₈, CTS₂₅, CTS₂₄ and CTS₁₈) was analyzed by XRD and the powder patterns of montmorillonite and organoclay are presented in Fig. 1. Since chitosan is polycationic in acidic environments, it can easily be adsorbed onto the negatively charged surface of the montmorillonite where cationic-exchange between the cationic chitosan and Na⁺ and Ca⁺ ions residing in the interspacing layer can take place [21]. The typical diffraction peak of montmorillonite was 6.06°, corresponding to a basal spacing of 14.59 Å. After modification of montmorillonite with depolymerized chitosan, the diffraction peak of original montmorillonite at 2θ = 6.06° disappeared and was substituted by a new diffraction peak around 2θ = 5.68°, 5.62°, 4.72°, 4.24° and 3.92°, corresponding to a basal spacing of 15.56, 15.73, 18.72, 20.84 and 22.54 Å, for organoclay with CTS_{initial}, CTS₂₈, CTS₂₅, CTS₂₄ and CTS₁₈, respectively. The movement of the typical diffraction peak of montmorillonite to lower angle indicated that the formation flocculated-intercalated nanostructure. It is reported that the flocculated structure in organoclay is due to the hydroxylated edge-edge interaction of the silicate layers [22]. The intensity of the peak decreased and even disappeared with decreasing of molecular weight of chitosan for montmorillonite modification indicated the formation of an intercalated-exfoliated structure in organoclay. The modification with CTS₁₈ shifted the montmorillonite diffraction peak to a lower angle indicating that the small polymer chains of chitosan18 had a higher ability to separate the montmorillonite layers than that of the larger sized chitosans. Therefore, organoclay formed by the modification of montmorillonite with CTS₁₈ provided the highest disordered interacted or nearly exfoliated montmorillonite particles and was used to form composite beads with CTS₁₈.

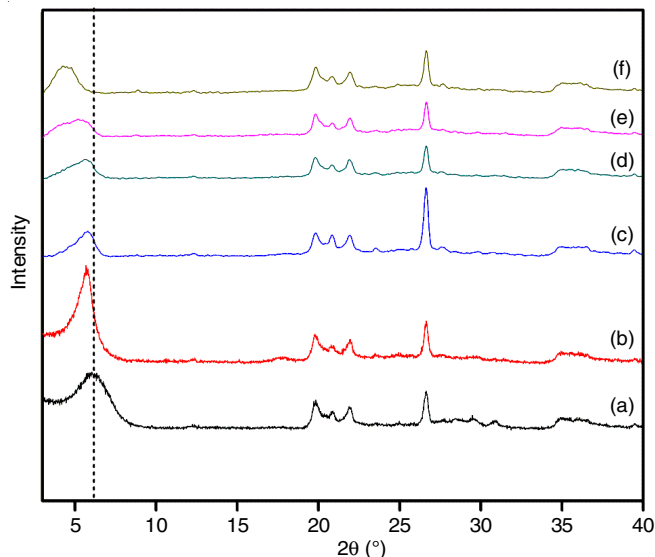


Fig. 1. XRD powder patterns of (a) original montmorillonite and organoclay with (b) CTS_{initial}, (c) CTS₂₈, (d) CTS₂₅, (e) CTS₂₄ and (f) CTS₁₈

Characterization of the adsorbents: The organoclay particles are uniformly distributed throughout the chitosan/organoclay nanocomposite beads. The porosity (ϵ) of the adsorbents was determined by the amount of water within the pores of the adsorbents [23]. The porosity (ϵ) can be calculated using these equations:

$$\epsilon = \frac{(W_w - W_D) / \rho_w}{W_D / \rho_{Mat} + (W_w - W_D) / \rho_w} \times 100 \% \quad (2)$$

where W_w (g) is the wet weight of the adsorbent beads before drying; W_D (g) is the wet weight of the beads after drying; ρ_w is the density of water, 1.0 g cm⁻³ and ρ_{Mat} is the density of adsorbent beads.

The general properties of chitosan and chitosan/organoclay nanocomposite beads are shown in Table-2. The water content of chitosan/organoclay nanocomposite beads less than that of chitosan beads, indicating that addition of organoclay made the beads materially denser. The density of the chitosan/modified montmorillonite nanocomposite beads was significantly higher than that of the chitosan beads due to the presence of organoclay. In addition, porosity in the chitosan/organoclay nanocomposite beads increased after the addition of organoclay into the beads, while the diameter of chitosan/organoclay nanocomposite beads less than that of chitosan beads.

SEM is a widely used technique to study the morphological and surface features of the adsorbent. In this study, SEM was used to assess morphological changes in chitosan surface after modification with organoclay. Fig. 2 (a) and (c) shows the SEM image of the chitosan and chitosan/organoclay nanocomposite beads, respectively. It is visible from micrographs

TABLE-1
MOLECULAR WEIGHT AND POLYDISPERSITY OF DEPOLYMERIZED CHITOSANS

Condition	Label	\bar{M}_w	\bar{M}_n	Polydispersity
No treatment	CTS _{initial}	150,000	50,000	3.5
10 % (v/v) H ₂ O ₂ for 12 h	CTS ₂₈	28,000	8,900	2.9
10 % (v/v) H ₂ O ₂ for 24 h	CTS ₂₅	25,000	8,400	3.3
20 % (v/v) H ₂ O ₂ for 12 h	CTS ₂₄	24,000	7,600	3.2
20 % (v/v) H ₂ O ₂ for 24 h	CTS ₁₈	18,000	5,700	2.8

TABLE-2
GENERAL PROPERTIES OF CHITOSAN AND CHITOSAN/ORGANOCLAY NANOCOMPOSITE BEADS

Adsorbent	Wet weight (W _w , g)	Dry weight (W _d , g)	Water content (%)	Density (g cm ⁻³)	Porosity (ε, %)	Diameter (D, mm)
Chitosan	4.61	0.38	91.76	3.84	76.77	4.08
Chitosan/organoclay-1	3.03	0.25	91.74	4.89	77.87	4.17
Chitosan/organoclay-2	3.39	0.29	91.44	5.76	81.79	4.37
Chitosan/organoclay-3	4.08	0.34	91.67	6.91	84.04	4.38
Chitosan/organoclay-4	3.48	0.30	91.38	7.78	87.60	4.67
Chitosan/organoclay-5	4.22	0.35	91.71	8.56	94.62	4.71

that organoclay particles were almost uniformly distributed in the chitosan matrix.

EDX spectroscopy was used to map the surface of the adsorbent in order to assess the adsorption sites containing adsorbed metal ions and their distribution along the surface of the adsorbent. Supplementary Fig. 2 (b) and (d) show the distribution of Ag(I) ions on the surface of the chitosan and chitosan/organoclay nanocomposite adsorbent. As can be seen in Supplementary Fig. 2 (b) and (d), a distribution of Ag(I) ions was observed on the surface of chitosan/organoclay nanocomposite adsorbent more densely than that of chitosan bead. This result suggests that the adsorbed of composite bead is governed by electrostatic forces.

Adsorption studies: Contact time studies are helpful in understanding the amount of Ag(I) ions adsorbed at various time intervals by a fixed amount of the adsorbents (1 g) at various concentration of organoclay in beads 1, 2, 3, 4 and 5

wt %. Fig. 3 clearly indicates a rapid increase in the amount of percentage removal with chitosan and chitosan/organoclay nanocomposite beads increased quickly in 30 min and then became slow and reached the maximum value at 150 min. This observation could be explained as at the beginning of the adsorption process, abundant binding sites were available on the surface of adsorbents, which make the adsorption process easier. Although at higher contact time, the rate of adsorption decreased and a saturation stage was attained due to the accumulation of the adsorption sites by the Ag(I) ions. This decline was due to decreased in total adsorbent surface area and increased diffusion pathway.

The percentage removal of Ag(I) ions increased with increasing organoclay concentration from 1 to 5 wt % in chitosan/organoclay nanocomposite beads (where chitosan concentration in beads was fixed at 2 wt %). The percentage of Ag(I) ions removal was increased proportionally with increasing

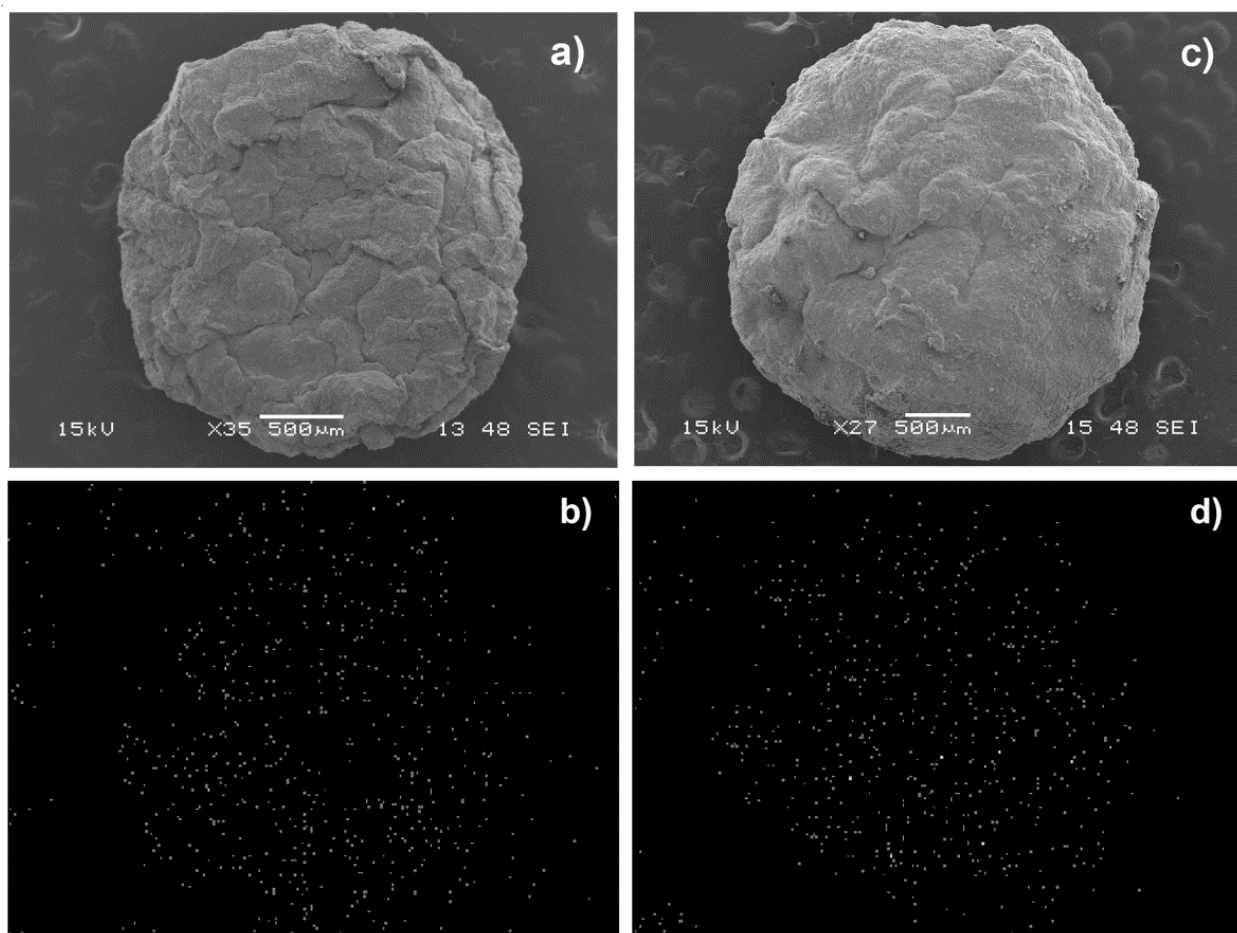


Fig. 2. SEM images and EDX mapping of (a-b) chitosan and (c-d) chitosan/organoclay nanocomposite beads after Ag(I) ions adsorption

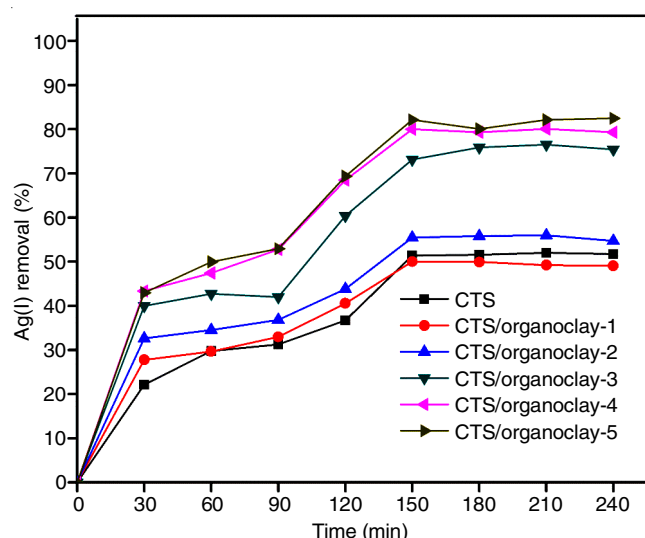


Fig. 3. Effects of contact time and organoclay concentration in beads on Ag(I) ions removal (adsorbent dosage 1 g, Ag(I) concentration 10 mg L⁻¹, volume 100 mL, pH 7)

organoclay concentration from 0 wt % (58.32 %) to 5 wt % (82.11 %) at 150 min. Organoclay has a negatively charged surface group and consequently increase in organoclay concentration in beads increased the adsorption of Ag(I) ions due to enhanced electrostatic interaction.

The pH of the aqueous solution is an important variable, it is well known that pH influences the adsorption processes significantly by affecting both the protonation of the surface groups and the degree of the ionization of the adsorbates [24]. Chitosan and chitosan/organoclay nanocomposite beads were slightly soluble in aqueous solution with a pH value of 3, so the range of pH for Ag(I) ions adsorption test selected in this study was between 4 and 10.

As shown in Fig. 4, the percentage removal of chitosan and chitosan/organoclay nanocomposite increase as the solution pH becomes less acidic from pH 4 to 6. The low uptake of Ag(I) ions at lower pH can be attributed to the high concentration of H⁺ ions, which compete against Ag(I) ions for the binding sites on the chitosan and chitosan/organoclay nanocomposite surface. In addition, most of the amino groups of chitosan and chitosan/organoclay nanocomposite become protonated (-NH₃⁺) at lower pH, which reduces the available binding sites for Ag(I) ions [25,26]. As Ag(I) ions are transported from the solution to the adsorbent, the protonated amino groups inhibit the approach of Ag(I) ions due to the electrostatic repulsion force exerted by NH₃⁺ on the adsorbent surface [27]. When the pH is increased from pH 4 to 6, the amino groups become deprotonated, due to free interaction and binding with Ag(I) ions. Therefore, the maximum adsorption of Ag(I) ions is observed at pH 6 on these two adsorbents. However, at pH values above 6, as insoluble silver hydroxide starts to precipitate from solution and range, both adsorption and precipitation are to be effective mechanisms in the removal of Ag(I) ions from aqueous solution. At this stage, it is worth pointing out that the Ag(I) ions removal of the nanocomposite is higher than the mean values of those of chitosan at any pH, which help to reduce the market cost of chitosan.

The effect of adsorbent dosage on the Ag(I) ions removal is presented in Fig. 5. These data was studied under the optimum

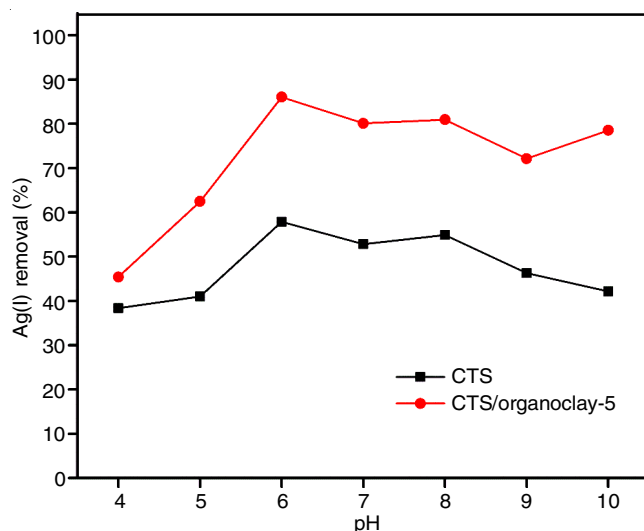


Fig. 4. Effects of pH on Ag(I) ions removal (adsorbent dosage 1 g, Ag(I) concentration 10 mg L⁻¹, volume 100 mL, contact time 150 min)

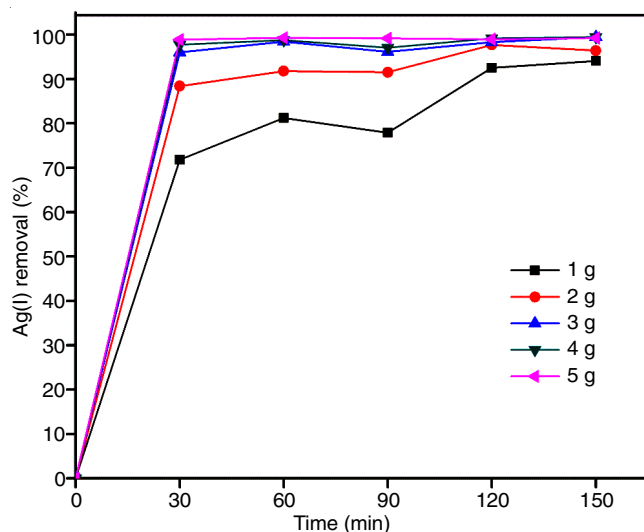


Fig. 5. Effect of adsorbent dosage on Ag(I) ions removal (chitosan/organoclay-5, pH 6, Ag(I) concentration 10 mg L⁻¹, volume 100 mL, contact time = 150 min)

batch conditions (initial metal concentration 10 mg L⁻¹, initial pH 6, contact time 150 min and concentration of organoclay 5 wt %). The result shows that the adsorbent dosage has an important role in the adsorption process. From the figure, it was observed that the percentage removal of the metal ions increases with increasing the adsorbents doses from 1 g to 3 g and further increase of the adsorbent doses did not provide more increment in the percentage of the metal ions removal. The increase in the percentage of the Ag(I) ions removal with increase in adsorbent dose is due to the greater availability of the surface area at higher concentration of the adsorbent [28]. Non-significant increase observed when the adsorbent doses were increased from 3 g to 5 g, suggests that after a certain dose of adsorbent, the maximum adsorption is attained and the amount of ions bound to the adsorbent and the amount of free ions remains constant even with further addition of the dose of adsorbent. In addition, the time required to reach equilibrium decreases at higher doses of adsorbent. This is due to the increase of efficient adsorption sites at higher dosages.

Adsorption isotherms: The adsorption isotherm models are used to describe the surface properties and affinity of adsorbent and to evaluate the adsorption capacity of the adsorbent. In this study, the two adsorption isotherm models, Langmuir and Freundlich isotherm models were selected to fit the equilibrium data obtained changing the initial concentration of the Ag(I) ions solution from 2 to 10 mg L⁻¹ under the optimal batch conditions as described earlier.

The Langmuir model is a valid monolayer adsorption on adsorbent surface containing a finite number of binding sites adsorbent [29]. The linear form of the Langmuir isotherm is expressed as:

$$\frac{C_e}{q_e} = \left(\frac{1}{bX_m} \right) + \left(\frac{C_e}{X_m} \right) \quad (3)$$

where q_e is the amount of metal ions adsorbed per unit mass of adsorbent (mg g⁻¹) and C_e is the equilibrium concentration of metal ions solution (mg L⁻¹). The constant X_m is the monolayer adsorption capacity (mg g⁻¹) and b is the Langmuir constant. The Langmuir isotherms of chitosan and chitosan/organoclay nanocomposite beads are shown in Fig. 6. The correlation coefficient (R^2) was found to be 0.998 and 0.989 for chitosan and chitosan/organoclay nanocomposite beads, respectively, indicating that the linear Langmuir model gives a good fit to the adsorption of Ag(I) ions onto chitosan and chitosan/organoclay nanocomposite adsorbents. The maximum adsorption capacity (X_m) of chitosan and chitosan/organoclay nanocomposite beads was found to be 46.83 and 80.39, respectively (Table-3). The increase in the adsorption capacity is due to high negative surface charge of organoclay.

Table-4 shows the maximum Ag(I) ions adsorption capacity of chitosan and chitosan/organoclay nanocomposite beads have been compared to other adsorbents. From this table, it can be

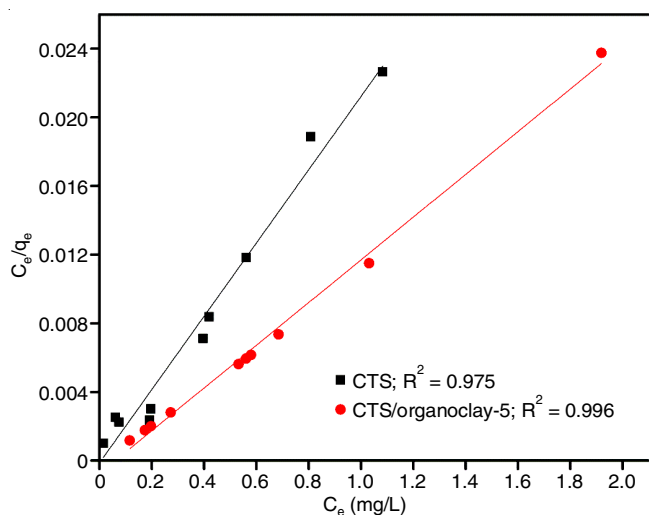


Fig. 6. Langmuir adsorption isotherm for the adsorption of Ag(I) ions onto chitosan and chitosan/organoclay nanocomposite beads

TABLE-4
COMPARISON OF Ag(I) ION ADSORPTION CAPACITY OF CHITOSAN/ORGANOCLAY NANOCOMPOSITE WITH THAT OF DIFFERENT ADSORBENTS

Adsorbent	Adsorption capacity (mg g ⁻¹)	Reference
Rice husk	1.62	[34]
Immobilized crab shell beads	2.95	[35]
Expanded perlite	8.46	[1]
Zeolite	33.23	[36]
Vermiculite	46.2	[37]
Modified bentonite clay	55.55	[38]
Chitosan/organoclay nanocomposite	80.39	This study
Activated carbon nanospheres	152	[39]
Mesoporous graphitic carbon nitride	400	[40]

concluded that the adsorption of Ag(I) ions onto chitosan/organoclay nanocomposite bead is effective as much as other adsorbents. In addition, the low cost, renewable, biodegradable and relatively non-toxic properties of chitosan/organoclay nanocomposite adsorbent make it to be promising adsorbent for the removal of Ag(I) ions from aqueous solution.

The Freundlich model is a non-ideal multilayer adsorption performed on heterogeneous surface [30]. This model can be written:

$$\log q_e = \frac{1}{n} \log C_e + \log K \quad (4)$$

where K is the Freundlich adsorption constant related to the adsorption capacity of adsorbent, $1/n$ is the adsorption intensity, which gives an indication of the favourability of adsorption. The Freundlich isotherms of chitosan and chitosan/organoclay nanocomposite beads are shown in Fig. 7 and the parameter summarized in Table-3. The K parameter was found to be 1.24 and 1.52 for chitosan and chitosan/organoclay nanocomposite beads, respectively, as n parameter was found to be 1.18 and 1.40, respectively. The values of n greater than 1 indicating that the adsorption of Ag(I) ions by using chitosan and chitosan/organoclay nanocomposite adsorbents was favourable at optimized conditions. Moreover, the R^2 values (0.937 for chitosan and 0.958 for chitosan/organoclay nanocomposite beads) was not able to express the association satisfactorily between the amount of the adsorbed Ag(I) ions (q_e) and the equilibrium concentration of Ag(I) ions solution (C_e).

Adsorption kinetics: Kinetics study plays a central role for the evaluation of an adsorption process and consists in the analysis of the mechanism involved in the solute uptake rate [31]. To describe the adsorption kinetics for a liquid-solid adsorption system, several models were formulated according to the process mechanism. For this purpose, the Lagergren's pseudo-first order and the pseudo-second order models were applied to the experimental data. The linear form of the pseudo-first order equation [32] is given as:

TABLE-3
LANGMUIR AND FREUNDLICH ISOTHERM PARAMETERS OBTAINED FROM THE ADSORPTION OF CHITOSAN AND CHITOSAN/ORGANOCLAY NANOCOMPOSITE (CONCENTRATION OF ORGANOCLAY 5 wt %) BEADS FOR Ag(I) IONS

Adsorbent	Langmuir isotherm			Freundlich isotherm		
	b (L mg ⁻¹)	X_m (mg g ⁻¹)	R^2	n	K (min ⁻¹)	R^2
Chitosan	2.14	46.83	0.975	1.18	1.24	0.937
Chitosan/organoclay-5	1.24	80.39	0.996	1.40	1.52	0.958

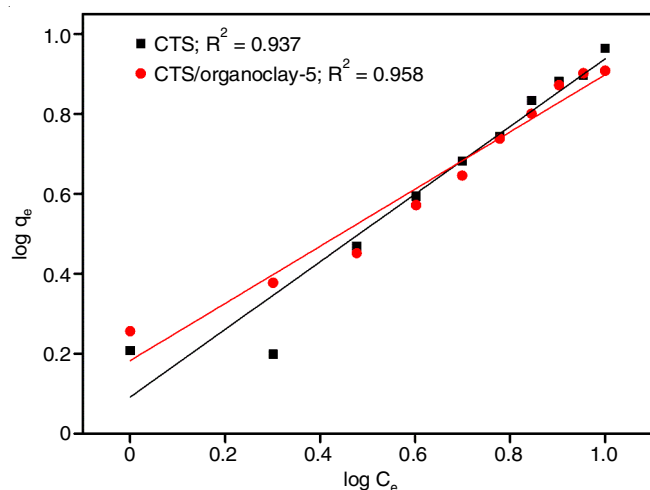


Fig. 7. Freundlich adsorption isotherm for the adsorption of Ag(I) ions onto chitosan and chitosan/organoclay nanocomposite beads

$$\log (q_e - q_t) = \log q_e - \frac{k_1}{2.303} t \quad (5)$$

where q_e and q_t (mg g^{-1}) are the amount of metal ions adsorbed at equilibrium time and any time (t), respectively. The k_1 parameter is the rate constant. Determined by plotting of $\log (q_e - q_t)$ and t . The q_e values, pseudo-first order rate constants and R^2 values are shown in Table-5. The adsorption of Ag(I) ions on chitosan/organoclay nanocomposite beads was not fitted to a pseudo-first order model and is shown in Fig. 8.

Pseudo-second order kinetic is expressed as the following equation [33]:

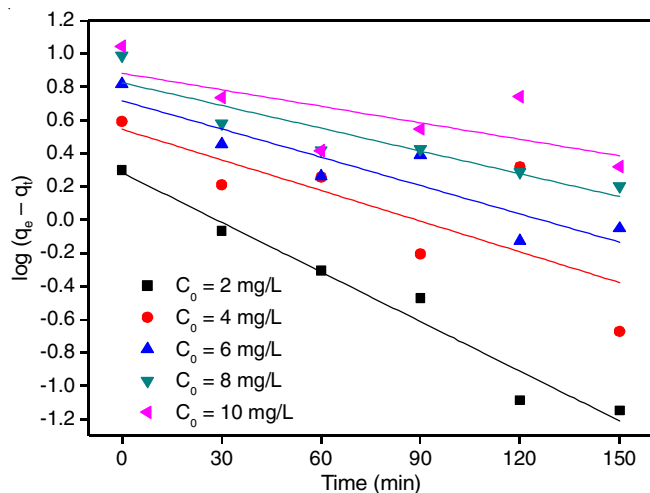


Fig. 8. Adsorption kinetic fitted by pseudo-first order equation for the adsorption of Ag(I) ions onto chitosan/organoclay nanocomposite beads

$$\frac{t}{q_t} = \frac{1}{k_2 q_e^2} + \frac{t}{q_e} \quad (6)$$

where q_e and q_t are the amount of metal ions (mg g^{-1}) adsorbed at equilibrium time and at time (t), respectively. The pseudo-second order kinetic for Ag(I) ions adsorption using chitosan/organoclay nanocomposite beads is presented in Fig. 9. The second order kinetic rate constant k_2 and correlation coefficients are presented in Table-5. The correlation coefficients for the second order kinetic model were higher than 0.90 indicating the applicability of this kinetic model of the adsorption process of Ag(I) ions on chitosan/organoclay nanocomposite beads.

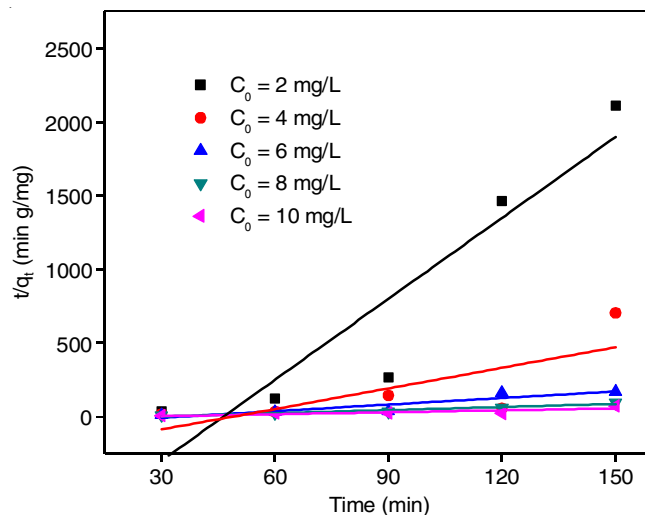


Fig. 9. Adsorption kinetic fitted by pseudo-second order equation for the adsorption of Ag(I) ions onto chitosan/organoclay nanocomposite beads

Desorption studies: The desorption studies are very important due to the economic success of the adsorption process depends on the regeneration of adsorbent. In this study the adsorption conditions was carried out at pH 6, 30 °C, contact time 150 min with initial Ag(I) concentration of 10 mg L⁻¹ and the desorption conditions were carried out at the pH range from 4 to 10, 30 °C and contact time 150 min. The effect of pH on desorption of Ag(I) ions from chitosan and chitosan/organoclay nanocomposite beads is shown in Fig. 10.

The contrast phenomenon from the adsorption was observed, revealing that the highest desorption percentage was in alkaline region. The results of the studies indicated that the desorption of the adsorbed Ag(I) ions in alkaline solution at pH 4 resulted in about 26.11 and 9.68 for chitosan and chitosan/organoclay nanocomposite beads, respectively. It is evident from the low desorption values that the adsorption of Ag(I)

TABLE-5
KINETIC PARAMETERS FOR THE ADSORPTION OF Ag(I) IONS ONTO CHITOSAN/ORGANOCLAY NANOCOMPOSITE BEADS BASED ON PSEUDO-FIRST AND PSEUDO-SECOND ORDER KINETIC EQUATIONS

C_0 (mg L^{-1})	Pseudo-first order			Pseudo-second order		
	q_e (mg g^{-1})	k_1 (min^{-1})	R^2	q_e (mg g^{-1})	k_2 ($\text{g mg}^{-1} \text{min}^{-1}$)	R^2
2	1.90	20.7×10^{-3}	0.95	0.06	0.49	0.97
4	3.61	14.2×10^{-3}	0.48	0.21	0.14	0.95
6	5.22	13.1×10^{-3}	0.79	0.34	0.09	0.96
8	6.60	10.5×10^{-3}	0.80	0.59	0.06	0.90
10	7.58	7.6×10^{-3}	0.37	0.83	0.04	0.95

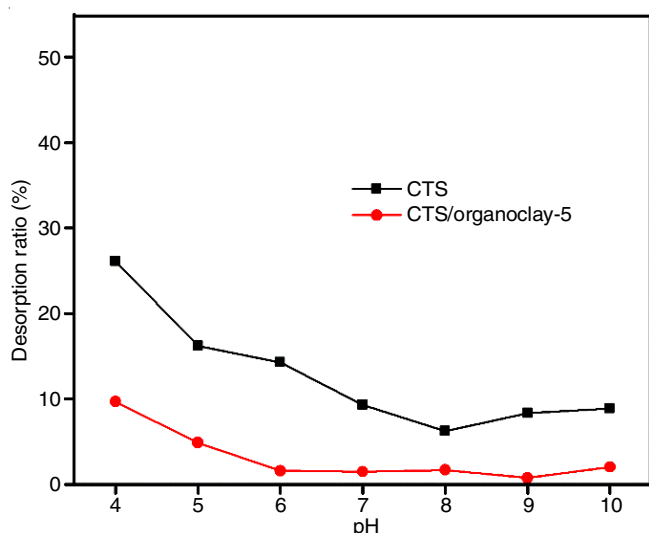


Fig. 10. Effects of pH on Ag(I) ions desorption ratio of chitosan and chitosan/organoclay nanocomposite beads (contact time = 150 min)

ions onto chitosan/organoclay nanocomposites was chemisorption in nature. Chemisorption exhibits poor desorption probably since the fact that in chemisorptions the adsorbate species are held firmly to the adsorbent with comparatively stronger bonds.

Conclusion

The aim of this study was to investigate the effect of chitosan with different polymer chain length (molecular weight) on the interlayer separation of montmorillonite to design Ag(I) ions adsorbents. The smaller sized chitosan slightly enlarged the interlayer separation. The modification of montmorillonite with CTS₁₈ led to the formation of intercalated or exfoliated montmorillonite particles as organoclay. CTS₁₈ imparted the highest basal spacing. Thus, organoclay was used to form nanocomposite beads with CTS_{initial} as an adsorbent for the Ag(I) ions from aqueous solution. The results indicated that the several factors such as contact time, organoclay concentration, pH value and adsorbent dosage affect the adsorption process. Isotherm analysis of the data showed that the adsorption pattern of Ag(I) ions onto nanocomposite followed well the Langmuir model. Using the Langmuir model equation, the maximum adsorption capacity of chitosan/organoclay nanocomposite bead was found 80.39 mg g⁻¹ for Ag(I) ions. The pseudo-second order equation described best the kinetic data of Ag(I) ions. Finally, it can be seen that the prepared adsorbent in this study shows good performance for Ag(I) ions adsorption, which might be related to the combination of the advantages of both chitosan and organoclay.

ACKNOWLEDGEMENTS

This research was supported by Office of Higher Education Research Promotion and National Research University under Office off the Higher Education Commission.

REFERENCES

- H. Ghassabzadeh, A. Mohadespour, M. Torab-Mostaedi, P. Zaheri, M.G. Maragheh and H. Taheri, *J. Hazard. Mater.*, **177**, 950 (2010).
- R. Ansari and A.F. Delavar, *J. Appl. Polym. Sci.*, **113**, 2293 (2009).
- H. Huo, H. Su and T. Tan, *Chem. Eng. J.*, **150**, 139 (2009).
- A.R. Nestic, S.J. Velickovic and D.G. Antonovic, *J. Hazard. Mater.*, **209-210**, 256 (2012).
- M. Zanetti, S. Lomakin and G. Camino, *Macromol. Mater. Eng.*, **279**, 1 (2000).
- L. Wang and A. Wang, *J. Hazard. Mater.*, **160**, 173 (2008).
- P. Monvisade and P. Siriphannon, *Appl. Clay Sci.*, **42**, 427 (2009).
- X. Ren, Z. Zhang, H. Luo, B. Hu, Z. Dang, C. Yang and L. Li, *Appl. Clay Sci.*, **97-98**, 17 (2014).
- D. Qin, X. Niu, M. Qiao, G. Liu, H. Li and Z. Meng, *Appl. Surf. Sci.*, **333**, 170 (2015).
- M. Ahmaruzzaman, *Adv. Colloid Interface Sci.*, **143**, 48 (2008).
- Y. Park, G.A. Ayoko and R.L. Frost, *J. Colloid Interface Sci.*, **360**, 440 (2011).
- V.K. Gupta and Suhas, *J. Environ. Manage.*, **90**, 2313 (2009).
- H. He, J. Duchet, J. Galy and J.F. Gérard, *J. Colloid Interface Sci.*, **295**, 202 (2006).
- Q. Zhou, R.L. Frost, H. He, Y. Xi and M. Zbik, *J. Colloid Interface Sci.*, **311**, 24 (2007).
- M. Cruz-Guzmán, R. Celis, M.C. Hermosín, W.C. Koskinen and J. Cornejo, *J. Agric. Food Chem.*, **53**, 7502 (2005).
- G. Yuan, *J. Environ. Sci. Health. Part A*, **39**, 2661 (2004).
- S. Bhowmick, S. Chakraborty, P. Mondal, W. Van Renterghem, S. Van den Berghe, G. Roman-Ross, D. Chatterjee and M. Iglesias, *Chem. Eng. J.*, **243**, 14 (2014).
- P. Baroni, R.S. Vieira, E. Meneghetti, M.G.C. da Silva and M.M. Beppu, *J. Hazard. Mater.*, **152**, 1155 (2008).
- L.M. Zhou, J.H. Liu and Z.R. Liu, *J. Hazard. Mater.*, **172**, 439 (2009).
- J. Iqbal, F.H. Wattoo, M.H.S. Wattoo, R. Malik, S.A. Tirmizi, M. Imran and A.B. Ghangro, *Arab. J. Chem.*, **4**, 389 (2011).
- M. Darder, M. Colilla and E. Ruiz-Hitzky, *Chem. Mater.*, **15**, 3774 (2003).
- S.S. Ray, K. Okamoto and M. Okamoto, *Macromolecules*, **36**, 2355 (2003).
- F. Zhao, B. Yu, Z. Yue, T. Wang, X. Wen, Z. Liu and C. Zhao, *J. Hazard. Mater.*, **147**, 67 (2007).
- E. Repo, J.K. Warchol, A. Bhatnagar and M. Sillanpää, *J. Colloid Interface Sci.*, **358**, 261 (2011).
- S.R. Popuri, Y. Vijaya, V.M. Boddu and K. Abburi, *Bioresour. Technol.*, **100**, 194 (2009).
- M.A. Salam, M.S.I. Makki and M.Y.A. Abdelaal, *J. Alloys Compd.*, **509**, 2582 (2011).
- L. Jin and R. Bai, *Langmuir*, **18**, 9765 (2002).
- M. Ahmaruzzaman and G.S. Laxmi, *Chem. Eng. J.*, **158**, 173 (2010).
- I. Langmuir, *J. Am. Chem. Soc.*, **40**, 1361 (1918).
- H.M.F. Freundlich, *J. Phys. Chem.*, **57**, 385 (1906).
- Y.S. Ho, *Scientometric*, **59**, 171 (2004).
- S. Lagergren, *Handlingar*, **24**, 1 (1898).
- Y.S. Ho and G. McKay, *Process Biochem.*, **34**, 451 (1999).
- S. Zafar, N. Khalid and M.L. Mirza, *Sep. Sci. Technol.*, **47**, 1793 (2012).
- C. Jeon, *J. Ind. Eng. Chem.*, **32**, 195 (2015).
- M. Akgül, A. Karabakan, O. Acar and Y. Yürüm, *Micropor. Mesopor. Mater.*, **94**, 99 (2006).
- A. Sari and M. Tüzen, *Micropor. Mesopor. Mater.*, **170**, 155 (2013).
- M.L. Cantuaria, A.F. Almeida Neto, E.S. Nascimento and M.G.A. Vieira, *J. Clean. Prod.*, **112**, 1112 (2016).
- X. Song, P. Gunawan, R. Jiang, S.S.J. Leong, K. Wang and R. Xu, *J. Hazard. Mater.*, **194**, 162 (2011).
- S.U. Lee, Y. Jun, E.Z. Lee, N.S. Heo, W.H. Hong, Y.S. Huh and Y.K. Chang, *Carbon*, **95**, 58 (2015).